Article

Genetic Diversity of *Diaphorina citri* and Its Endosymbiont Across Diffusion Frontier and Epidemic Areas of Citrus Huanglongbing in China

Jin Yang [1], Ai-Jun Huang [1,2], Jun Zhou [1,2], Ping You [1], Xiang Li [1], Han Luo [1] and Long Yi [1,2,*]

1   School of Life Science, Gannan Normal University, Ganzhou 341000, China; yangjin990527@163.com (J.Y.); hajgnnu@sina.com (A.-J.H.); 13102188352@163.com (J.Z.); yp961939590@163.com (P.Y.); x18317513414@163.com (X.L.); 18460323269@163.com (H.L.)
2   National Navel Orange Engineering Research Center, Ganzhou 341000, China
*   Correspondence: yilonggnnu@163.com

Abstract: Citrus huanglongbing (HLB) is one of the most severe diseases affecting the citrus industry, with *Diaphorina citri* (Hemiptera: Liviidae) serving as its primary natural vector. To understand the genetic diversity and population structure of *D. citri* in the context of HLB diffusion, we analyzed 13 populations from the HLB diffusion frontier and 25 populations from epidemic areas in China. The HLB diffusion frontier areas refer to the peripheral regions of HLB distribution in China, including the western Zhejiang, southern Jiangsu, northern Jiangxi, northern Hunan, and eastern Sichuan provinces. In contrast, the HLB epidemic areas represent regions in China where HLB is actively widespread and causing significant impacts. We utilized mitochondrial genes (*COI*, *ND5*, and *Cytb*) of *D. citri* and housekeeping genes (*dnaQ*, *rpoC*, and *argH*) of its endosymbiont *Candidatus* Carsonella ruddii (*Ca.* C. ruddii) for this analysis. Our findings revealed that the *D. citri* and *Ca.* C. ruddii in different regions showed low haplotype diversity and nucleotide diversity. While the genetic variation in *D. citri* populations primarily occurred within populations, the endosymbiont showed contrasting patterns in the HLB epidemic areas. We identified three dispersal paths: (1) migration of the Yunnan population to Sichuan, Guizhou, and Guangxi; (2) movement of the Guangdong population to Fujian, Jiangxi, and Zhejiang; and (3) dispersal of the Guangdong population to Hunan and Guangxi. Our study suggests that *D. citri* populations at the HLB diffusion frontier are predominantly transmitted from neighboring epidemic areas.

Keywords: citrus huanglongbing; *Diaphorina citri*; mitochondrial gene; endosymbionts; *Candidatus* Carsonella ruddii

1. Introduction

Citrus Huanglongbing (HLB), an extremely destructive bacterial disease, is caused by the Gram-negative bacterium *Candidatus* Liberibacter asiaticus (CLas), which acts as a phloem-localized parasite [1]. Based on differences in the 16S rRNA sequence and geographic distribution of the citrus HLB pathogen, it is categorized into three species: *Candidatus* Liberibacter asiaticus (CLas) [2], *Candidatus* Liberibacter africanus (CLaf) [3], and *Candidatus* Liberibacter americanus (CLam) [4,5]. Among these, CLas is the most widespread and destructive. It is found not only in Asia but also in the Americas, Africa, and the Middle East. In China, HLB is specifically caused by CLas [6]. The disease was first identified in Taipei, China, in 1913 [7], and later appeared on the Chinese mainland

in 1919 [8]. Today, it is prevalent in 10 provinces (autonomous regions) and 349 counties (cities and districts) across China [9,10].

Diaphorina citri (Hemiptera: Liviidae) primarily infests citrus and other Rutaceae plants. Infestations result in stunted tree growth in mild cases and plant mortality in severe cases. Furthermore, *D. citri* serves as the primary natural vector for citrus HLB transmission [11]. The pest was first recorded in Taiwan, China, in 1907 [12] and later in mainland China in 1934 [13]. Subsequently, *D. citri* was identified in Brazil in 1936 [14] and spread to Florida in the 1990s [15]. Currently, it is distributed across Asia, the Middle East, the southern United States, the Caribbean Islands, and Central and South America [16–22].

Understanding the genetic variation and population structure of *D. citri* in China provides crucial insights into its geographic origins and invasion pathways. This can offer valuable information for biological control and pest management programs [23]. Mitochondrial DNA analysis is a widely used method for phylogenetic and population genetic studies [24–27]. Compared with nuclear genes, mtDNA is a highly conserved maternal marker that is unaffected by life stage, polymorphism, or gender [28]. Zhang et al. [29] investigated potential invasion sources and dispersal routes of *D. citri* in China using mitochondrial genes *COI* and *Cytb*, identifying two possible origins in Guangdong and Yunnan, along with three dispersal pathways. In a separate study, Luo et al. [30] analyzed 356 *D. citri* populations from 106 regions worldwide using mitochondrial genes *COI*, revealing low nucleotide diversity but high haplotype diversity. Their findings suggested three transmission routes for *D. citri*: from South Asia to North America via West Asia, from Southeast Asia to East Asia, and from Southeast Asia to South America through Africa [30]. Additionally, Huang et al. [31] assessed the genetic diversity and population structure of *D. citri* in southwest, central, east, and south China using the mitochondrial genes *COI*. They found that the population in southwest China exhibited significantly greater differentiation compared to the other three regions [31]. These comprehensive studies enhance our understanding of *D. citri* dynamics and contribute to the development of effective pest management strategies. Cui et al. [32] conducted a phylogenetic analysis of the *D. citri* mitochondrial genome, revealing that *D. citri* from Leibo, Pingshan, and Xuzhou (rural areas) formed a distinct group (MG4), characterized by three unique SNPs in *cox1*, *nad4*, and *cytb*. In contrast, *D. citri* from Cuiping and Xuzhou (urban areas) clustered with the southeast China group. A study on the genetic diversity of *D. citri* in Puerto Rico revealed a unique haplotype in the Caribbean, which was more closely related to haplotypes from Southwest Asia than other regions. This suggested that the Caribbean invasion did not originate from the United States [33].

Endosymbionts are microorganisms that reside within insects for extended periods, forming a symbiotic relationship with their insect hosts. These microorganisms include bacteria, fungi, viruses, and small protists [34]. In the evolutionary context of insect biology, insect endosymbionts are categorized as primary or secondary endosymbionts [35]. Most insects host only one primary endosymbiont, establishing a strict symbiotic bond. For example, the primary endosymbiont of *D. citri* is *Ca.* C. ruddii [36]. Nakabachi et al. [37] were the first to sequence and annotate the genome of *Ca.* C. ruddii, an indigenous endosymbiont of *D. citri*, revealing a genome size of 159,622 bp, primarily comprising genes related to amino acid synthesis. Therefore, it is believed to function as a nutritional endosymbiont for *D. citri*, providing essential amino acids and other nutrients absent in its diet. Wang et al. [38] utilized mutation sites for population dynamics analysis of the geographical lineage of *D. citri*, focusing on the endosymbionts *Ca.* C. ruddii. By integrating mitochondrial genes, they unveiled the genetic evolutionary relationships among 24 geographical populations of *D. citri* across Asian countries and the United States. This study demonstrated the utility of *Ca.* C. ruddii in tracing the history of

population lineage diffusion in *D. citri* populations. Wu et al. [39] analyzed the population diversity of *D. citri* across 54 citrus-producing areas in 11 provinces in China. Diversity primarily arose from single nucleotide polymorphisms in five mitochondrial genes: *nad3*, *cox2*, *rrnL*, *cob*, and *atp6*. Nine SNPs grouped the mitochondrial genomes of *D. citri* into three main clusters, including seven subgroups. Additionally, the genomes of *D. citri* endosymbionts *Ca.* C. ruddii and *Candidatus* Profftella armatura were sequenced from 31 new samples in China, and independent phylogenetic trees were constructed, supporting the mitochondrial genome analysis. Zhang et al. [40] analyzed the genomes of 65 *Wolbachia* endosymbionts, classifying them into Asian and North American strains. Concurrently, the analysis confirmed that *D. citri* in Florida did not originate from China. This study provides valuable insights into the geographical distribution of Wolbachia, its host's origin, and the host–endosymbiont interaction. Endosymbionts of *D. citri* have been extensively used in host genetic analyses [41,42].

This study focused on *D. citri* in the diffusion frontier and epidemic areas of HLB. Using mitochondrial genes of *D. citri* (*COI*, *ND5*, and *Cytb*) and genes of its primary endosymbiont *Ca.* C. ruddii housekeeping genes (*dnaQ*, *rpoC*, and *argH*) as molecular markers, the genetic structure was examined. The aim was to provide robust evidence for analyzing the relationship between the geographical distribution and genetic lineage of *D. citri* in the HLB diffusion frontier and epidemic areas.

2. Materials and Methods

2.1. Sample Collection and DNA Extraction

Between 2021 and 2023, 1140 *D. citri* adults were collected from commercial and unmanaged citrus groves at 38 sites across southern China, a major region for *D. citri* occurrence. The coordinates of each sampling site were recorded using a portable GPS device (Zhuolin A6, Hefei, China) (Figure 1). Of these, two were from Fujian, four from Guangdong, four from Guangxi, two from Guizhou, six from Hunan, eight from Jiangxi, five from Sichuan, two from Yunnan, and five from Zhejiang. Based on the incidence of HLB, the collection sites were categorized into 13 HLB diffusion frontier areas and 25 epidemic areas were included in the study. The collected samples were preserved in 75% ethanol and stored at −20 °C until DNA extraction. Detailed information on sample collection by region is provided in Table 1.
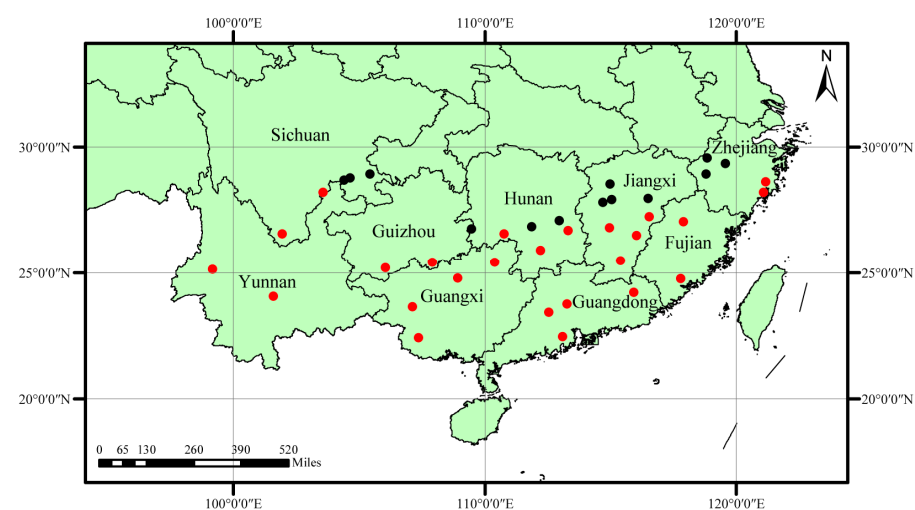

Figure 1. *D. citri* sampling sites. The black solid circle is the sampling location from the HLB diffusion frontier areas, and the red solid circle is the sampling location from the HLB epidemic areas.

Table 1. Localities, host, number of *D. citri* individuals (N), latitude and longitude in each sampled locality.

Populations	Localities	Host	N	Latitude and Longitude	Populations	Localities	Host	N	Latitude and Longitude
FJNP	Nanping, Fujian	*C. maxima*	30	N27.038°E117.879°	JXFY *	Fenyi, Jiangxi	*C. reticulata*	30	N27.807°E114.679°
FJZZ	Zhangzhou, Fujian	*C. maxima*	30	N24.747°E117.772°	JXLC *	Linchuan, Jiangxi	*C. limon*	30	N27.957°E116.487°
GDJM	Jiangmen, Guangdong	*C. reticulata*	30	N22.456°E113.069°	JXND	Ningdu, Jiangxi	*C. sinensis*	30	N26.487°E116.010°
GDMZ	Meizhou, Guangdong	*C. sinensis*	30	N24.202°E115.914°	JXNF	Nanfeng, Jiangxi	*C. reticulata*	30	N27.234°E116.528°
GDQY	Qingyuan, Guangdong	*C. reticulata*	30	N23.746°E113.264°	JXTH	Taihe, Jiangxi	*C. reticulata*	30	N26.805°E114.945°
GDZQ	Zhaoqing, Guangdong	*C. sinensis*	30	N23.425°E112.540°	JXYF *	Yifeng, Jiangxi	*C. reticulata*	30	N28.532°E114.961°
GXBS	Baise, Guangxi	*C. reticulata*	30	N23.629°E107.105°	JXYS *	Yushui, Jiangxi	*C. reticulata*	30	N27.914°E115.028°
GXCZ	Chongzuo, Guangxi	*C. sinensis*	30	N22.400°E107.354°	SCCP *	Cuiping, Sichuan	*C. sinensis*	30	N28.770°E104.625°
GXGL	Guilin, Guangxi	*C. reticulata*	30	N25.408°E110.371°	SCLS	Liangshan, Sichuan	*C. sinensis*	30	N28.209°E103.556°
GXHC	Hechi, Guangxi	*C. reticulata*	30	N24.781°E108.910°	SCLZ *	Luzhou, Sichuan	*C. sinensis*	30	N28.916°E105.423°
GZQN	Qiannanzhou, Guizhou	*C. reticulata*	30	N25.423°E107.899°	SCPZH	Panzhihua, Sichuan	*C. sinensis*	30	N26.554°E101.934°
GZQXN	Qianxinanzhou, Guizhou	*C. reticulata*	30	N25.206°E106.028°	SCXZ *	Xuzhou, Sichuan	*C. reticulata*	30	N28.693°E104.387°
HNCZ	Chenzhou, Hunan	*C. sinensis*	30	N26.685°E113.292°	YNBS	Baoshan, Yunnan	*C. reticulata*	30	N25.130°E99.175°
HNHD *	Hengdong, Hunan	*C. sinensis*	30	N27.079°E112.948°	YNYX	Yuxi, Yunnan	*C. reticulata*	30	N24.047°E101.576°
HNHH *	Huaihua, Hunan	*C. sinensis*	30	N26.750°E109.461°	ZJHZ *	Hangzhou, Zhejiang	*C. reticulata*	30	N29.557°E118.827°
HNQD *	Qidong, Hunan	*C. sinensis*	30	N26.839°E111.859°	ZJJH *	Jinhua, Zhejiang	*C. reticulata*	30	N29.332°E119.539°
HNSY	Shaoyang, Hunan	*C. sinensis*	30	N26.552°E110.755°	ZJQZ *	Quzhou, Zhejiang	*C. reticulata*	30	N28.928°E118.779°
HNYZ	Yongzhou, Hunan	*C. sinensis*	30	N25.904°E112.204°	ZJTZ	Taizhou, Zhejiang	*C. reticulata*	30	N28.625°E121.147°
JXAY	Anyuan, Jiangxi	*C. sinensis*	30	N25.482°E115.375°	ZJWZ	Wenzhou, Zhejiang	*C. reticulata*	30	N28.209°E121.067°

Note: Asterisks indicate *D. citri* populations in the diffusion frontier areas of HLB.

2.2. DNA Extraction, PCR, and Sequencing

Whole-genome DNA was extracted from individual specimens using the DNeasy Blood and Tissue Kit (Qiagen, Valencia, CA, USA) following the manufacturer's protocol. The mitochondrial genes *COI* of *D. citri* was amplified as described by Boykin et al. [19], while the *Cytb* primers were obtained from Zhang et al. [29]. Primers for *ND5* were designed based on available complete mitochondrial genome sequences of *D. citri*. The primer sequence for *Ca.* C. ruddii housekeeping genes (*dnaQ*, *rpoC*, and *argH*) was adopted from Wang et al. [38]. Details of primer fragment names and sequences are provided in Table 2.

Table 2. Primers used for the amplification and sequencing.

Species	Fragment	Primer	Sequence (5′-3′)	Tm (°C)	Reference
D. citri	*COI*	*COI*-F *COI*-R	AGGAGGTGGAGACCCAATCT TCAATTGGGGGAGAGTTTTG	56	[19]
	Cytb	*Cytb*-F *Cytb*-R	CGAGATGTAAATAATGGGTG TAGGGAATTTCAACAGGTTT	56	[29]
	ND5	*ND5*-F *ND5*-R	TTTTTGACCCAGCTACTCAT GATTTTTAGTCCGAGCATTG	56	This study
Ca. C. ruddii	*dnaQ*	*dnaQ*-F *dnaQ*-R	TGAAACAACAGGTTTATCACCACA CCAAGCATCTAAAATAGCTGTATGT	56	[38]
	rpoC	*rpoC*-F *rpoC*-R	TGAAGAGTTGGGGCTCTATTCA GGAATTCCTCATGTTGATTCAGGT	64	
	argH	*argH*-F *argH*-R	CTCCTATGCCTGGATTTACTCA TTGATTAGGCGCTGTACCTCC	56	

The polymerase chain reaction (PCR) mixture comprised 10.5 µL of nuclease-free water, 12.5 µL of 2× Taq PCR MasterMix II (TaKaRa Co., Dalian, China), 0.5 µL each of forward and reverse primers (10 µM), and 1 µL of DNA template (50–200 ng/µL), resulting in a total reaction volume of 25 µL. Amplifications were performed using a Veriti 96-well thermal cycler (Applied Biosystems, Foster City, CA, USA) under the following conditions: initial denaturation at 95 °C for 3 min; 35 cycles of 95 °C for 30 s, annealing at the specific temperature (Tm) for 1 min, and extension at 72 °C for 1 min; followed by a final extension at 72 °C for 10 min.

All amplified products were subjected to electrophoresis on a 1.2% agarose gel. The length of the target bands was determined using DL 2000 (TaKaRa Co., Dalian, China) as a reference marker, and a single product with clear bands was selected for sequencing at Sangon Biotech (Shanghai, China).

2.3. Genetic Diversity and Genetic Structure

To analyze the genetic diversity of *D. citri* populations, we used various bioinformatics tools and statistical methods. First, we employed SeqMan 7.1.0 [43] to assemble and manually correct the sequenced data. The clipped and spliced sequences were then aligned using ClustalW in MEGA 7.0 [44]. Genetic diversity parameters, including base composition, the proportion of bases, the number of polymorphic sites (S), synonymous (Ks) and non-synonymous (Ka) substitution rates, haplotype diversity (Hd), haplotype number (H), and nucleotide diversity (π), were calculated using DnaSP 5.0 [45]. A mismatch analysis was performed, and the data were visualized in Excel 2020. To assess genetic differentiation between *D. citri* populations, pairwise *Fst* values were calculated and a molecular analysis of variance (AMOVA) was performed across 38 geographic regions using Arlequin 3.5 [46].

Fst values were interpreted as follows: $0 < Fst \leq 0.05$ for mild genetic differentiation, $0.05 < Fst \leq 0.15$ for moderate differentiation, $0.15 < Fst \leq 0.25$ for high differentiation, and $Fst > 0.25$ for severe differentiation. To infer the phylogenetic relationships among haplotypes, after screening the HKY's best model, a maximum likelihood (ML) tree with 1000 bootstrap replicates was constructed using MEGA 7.0. The haplotype network was visualized using the Templeton, Crandall, and Sing (TCS) method [47] in PopART 1.7 [48]. To investigate the correlation between genetic and geographic distance, we conducted principal coordinate analysis (PCoA) and Mantel tests (10,000 permutations) [49] using GenAlEx v.6.5 [50]. Furthermore, neutral tests, including Tajima's *D* [51], Fu and Li's *D*, and Fu and Li's *F* [52] tests were performed using DnaSP to examine evidence of historical population expansion.

3. Results

3.1. Genetic Diversity and Population Structure of D. citri

In this study, the mitochondrial multi-gene concatenated sequences of *D. citri* was 2251 bp, consisting of *COI* (725 bp), *ND5* (794 bp), and *Cytb* (732 bp). In the dataset of 1140 sequences from 38 regions, the A + T content was 68.90%, indicating a significant A + T bias. A total of 81 polymorphic loci were identified, including 39 parsimony-informative loci and 42 single-variation loci. Among the analyzed sequences, 82 haplotypes (designated H1 to H82) were identified (Table 3). Notably, 18 haplotypes were shared across two or more populations, while 64 were exclusive to a single population. The most prevalent haplotype, H1, accounted for 66.49% of the total samples (758 sequences) and was found in all populations except GZQXN, SCLS, and YNBS. H63 (4.82%, 55 sequences) and H23 (4.65%, 53 sequences) were the second and third most common haplotypes.

High Hd (0.551 ± 0.018) and low π (0.00039 ± 0.00002) were observed, with a mean nucleotide difference (k) of 0.883. Certain populations, such as FJZZ (0.766), GXBS (0.630), GXCZ (0.745), GXGL (0.570), JXLC (0.515), JXNF (0.726), JXYS (0.591), SCPZH (0.540), YNBS (0.729), and YNYX (0.770), exhibited high Hd (Table 3). The non-synonymous (Ka) to synonymous (Ks) substitution rate ratios, which assess selection pressure at the protein level, revealed Ka/Ks values > 1 (12.92).

Genetic analysis revealed that haplotypes from all populations could be categorized into two groups, i.e., Groups A and B (Figure 2a). Group A comprises 64 haplotypes, with H1 being the most prevalent. Group B is further subdivided into two subgroups: BI and BII. BI consists of nine haplotypes (H4, H10, H18, H26, H30, H45, H70, H73, and H81), distributed across all sampled provinces in this study. BII also contains nine haplotypes (H16, H36, H39, H65, H66, H67, H71, H72, and H74), primarily found in four regions: Guangdong, Hunan, Zhejiang, and Guangxi. However, there were other regions, including Yunnan, Guizhou, and Sichuan. PCoA analysis (Figure 2b) demonstrated that while some *D. citri* from different populations showed widely varying distributions, most populations exhibited overlapping distributions. The populations can be categorized into three groups: (1) YNBS, FJZZ, GDZQ, HNCZ, ZJTZ, and SCPZH; (2) YNBS, YNYX, SCPZH, and GZQN; and (3) other populations, corresponding to lineages BI, BII, and A, respectively.

The haplotype network, constructed using the TCS inference method, is divided into two subregions. The network exhibits a star-shaped pattern, with the most frequent haplotype, H1, at the central position. All other haplotypes are derived through one or a few mutation steps (Figure 3).

Table 3. Haplotype (Hap), haplotype diversity (Hd), and nucleotide diversity (π) in each sampled locality.

Populations	Hap	Hd	π	Hap	Hd	π
	D. citri			*Ca.* C. ruddii		
FJNP	H1(23), H2(3), H3(1), H4(2), H5(1)	0.409 ± 0.108	0.00020 ± 0.00006	C1(9), C2(17), C3(3), C4(1)	0.598 ± 0.068	0.00029 ± 0.00005
FJZZ	H1(7), H4(13), H6(1), H7(2), H8(2), H9(2), H10(1), H11(1), H12(1)	0.766 ± 0.063	0.00066 ± 0.00010	C1(1), C2(25), C5(2), C6(1)), C7(1)	0.308 ± 0.107	0.00014 ± 0.00005
GDJM	H1(29), H13(1)	0.067 ± 0.061	0.00006 ± 0.00005	C1(20), C8(10)	0.460 ± 0.061	0.00038 ± 0.00005
GDMZ	H1(29), H14(1)	0.067 ± 0.061	0.00003 ± 0.00003	C1(16), C2(14)	0.515 ± 0.027	0.00021 ± 0.00001
GDQY	H1(27), H15(2), H16(1)	0.191 ± 0.093	0.00009 ± 0.00004	C1(27), C2(2), C9(1)	0.191 ± 0.093	0.00008 ± 0.00004
GDZQ	H1(22), H15(1), H17(2), H18(1), H19(1), H20(1), H21(1), H22(1)	0.467 ± 0.112	0.00023 ± 0.00007	C1(24), C10(1), C11(3), C12(2)	0.356 ± 0.106	0.00034 ± 0.00012
GXBS	H1(15), H15(1), H23(11), H24(2), H25(1)	0.630 ± 0.058	0.00033 ± 0.00005	C1(8), C2(17), C13(1), C14(1)), C15(2), C16(1)	0.621 ± 0.077	0.00031 ± 0.00005
GXCZ	H1(13), H23(8), H26(3), H27(1), H28(2), H29(1), H30(2)	0.745 ± 0.059	0.00055 ± 0.00009	C1(7), C2(17), C17(6)	0.605 ± 0.066	0.00029 ± 0.00004
GXGL	H1(19), H5(6), H30(2), H31(1), H32(1), H33(1)	0.570 ± 0.092	0.00029 ± 0.00006	C1(22), C2(6), C14(1), C18(1)	0.434 ± 0.095	0.00021 ± 0.00005
GXHC	H1(22), H16(3), H30(3), H34(1), H35(1)	0.455 ± 0.106	0.00022 ± 0.00006	C1(24), C2(3), C10(1), C19(1), C20(1)	0.359 ± 0.108	0.00016 ± 0.00005
GZQN	H1(22), H23(1), H27(1), H30(1), H36(3), H37(1), H38(1)	0.462 ± 0.110	0.00034 ± 0.00010	C1(16), C2(3), C20(2), C21(2), C22(3), C23(1), C24(2), C25(1)	0.703 ± 0.085	0.00060 ± 0.00012
GZQXN	H23(30)	0.000 ± 0.000	0.00000 ± 0.00000	C2(30)	0.000 ± 0.000	0.00000 ± 0.00000
HNCZ	H1(26), H39(1), H40(1), H41(2)	0.251 ± 0.102	0.00012 ± 0.00005	C1(27), C10(1), C26(1), C27(1)	0.193 ± 0.095	0.00008 ± 0.00004
HNHD *	H1(28), H42(2)	0.129 ± 0.079	0.00006 ± 0.00004	C1(30)	0.000 ± 0.000	0.00000 ± 0.00000
HNHH *	H1(24), H30(3), H43(2), H44(1)	0.356 ± 0.106	0.00017 ± 0.00006	C1(25), C2(3), C28(2)	0.301 ± 0.102	0.00013 ± 0.00005
HNQD *	H1(25), H16(2), H30(3)	0.301 ± 0.102	0.00014 ± 0.00005	C1(26), C2(4)	0.239 ± 0.092	0.00010 ± 0.00004
HNSY	H1(26), H30(4)	0.239 ± 0.092	0.00011 ± 0.00004	C1(22), C2(4), C18(2), C29(1), C30(1)	0.453 ± 0.105	0.00033 ± 0.00010
HNYZ	H1(25), H30(1), H35(1), H45(1), H46(1), H47(1)	0.310 ± 0.109	0.00018 ± 0.00007	C1(26), C2(4)	0.239 ± 0.092	0.00010 ± 0.00004
JXAY	H1(22), H4(1), H17(1), H47(2), H48(1), H49(2), H50(1)	0.464 ± 0.111	0.00029 ± 0.00009	C1(24), C2(3), C31(2), C32(1)	0.356 ± 0.106	0.00020 ± 0.00007
JXFY *	H1(24), H15(3), H17(1), H51(1), H52(1)	0.359 ± 0.108	0.00017 ± 0.00006	C1(23), C2(1), C33(3), C34(1), C35(2)	0.409 ± 0.108	0.00019 ± 0.00006
JXLC *	H1(14), H47(16)	0.515 ± 0.027	0.00023 ± 0.00001	C1(25), C2(5)	0.287 ± 0.092	0.00012 ± 0.00004

Table 3. *Cont.*

Populations	Hap	Hd	π	Hap	Hd	π
	D. citri			*Ca.* C. ruddii		
JXND	H1(30)	0.000 ± 0.000	0.00000 ± 0.00000	C1(24), C36(6)	0.331 ± 0.089	0.00014 ± 0.00004
JXNF	H1(15), H47(5), H53(1), H54(2), H55(1), H56(1), H57(3), H58(1), H59(1)	0.726 ± 0.077	0.00069 ± 0.00013	C1(25), C14(3), C37(1), C38(1)	0.303 ± 0.104	0.00021 ± 0.00010
JXTH	H1(25), H4(1), H35(1), H42(1), H60(1), H61(1)	0.310 ± 0.109	0.00015 ± 0.00006	C1(26), C2(2), C39(2)	0.248 ± 0.100	0.00011 ± 0.00004
JXYF *	H1(30)	0.000 ± 0.000	0.00000 ± 0.00000	C1(24), C2(2), C40(1), C41(2), C42(1)	0.361 ± 0.109	0.00018 ± 0.00006
JXYS *	H1(17), H47(4), H62(9)	0.591 ± 0.064	0.00030 ± 0.00004	C1(12), C2(7), C43(1), C44(6), C45(1), C46(1), C47(2)	0.763 ± 0.050	0.00044 ± 0.00005
SCCP *	H1(30)	0.000 ± 0.000	0.00000 ± 0.00000	C1(1), C48(29)	0.067 ± 0.061	0.00003 ± 0.00003
SCLS	H63(30)	0.000 ± 0.000	0.00000 ± 0.00000	C18(9), C49(16), C50(4), C51(1)	0.628 ± 0.063	0.00040 ± 0.00004
SCLZ *	H1(24), H23(3), H30(1), H64(2)	0.356 ± 0.106	0.00017 ± 0.00006	C1(14), C2(14), C20(1), C52(1)	0.582 ± 0.045	0.00027 ± 0.00004
SCPZH	H1(3), H63(4), H65(20), H66(2), H67(1)	0.540 ± 0.099	0.00036 ± 0.00008	C1(2), C18(4), C22(22), C53(1), C54(1)	0.453 ± 0.105	0.00030 ± 0.00009
SCXZ *	H1(7), H63(21), H68(1), H69(1)	0.469 ± 0.089	0.00024 ± 0.00005	C10(22), C48(7), C55(1)	0.421 ± 0.087	0.00048 ± 0.00010
YNBS	H65(6), H70(14), H71(4), H72(4), H73(1), H74(1)	0.729 ± 0.063	0.00192 ± 0.00010	C22(7), C56(12), C57(1), C58(2), C59(5), C60(2), C61(1)	0.772 ± 0.052	0.00185 ± 0.00012
YNYX	H1(3), H36(6), H65(12), H72(6), H75(2), H76(1)	0.770 ± 0.050	0.00053 ± 0.00007	C2(5), C22(22), C62(2), C63(1)	0.444 ± 0.100	0.00036 ± 0.00009
ZJHZ *	H1(23), H16(4), H77(2), H78(1)	0.402 ± 0.104	0.00019 ± 0.00006	C1(1), C2(14), C64(2), C65(2), C66(5), C67(3), C68(2), C69(1)	0.754 ± 0.070	0.00050 ± 0.00007
ZJJH *	H1(28), H79(2)	0.129 ± 0.079	0.00006 ± 0.00004	C1(10), C2(10), C14(2), C66(7), C70(1)	0.743 ± 0.038	0.00045 ± 0.00005
ZJQZ *	H1(25), H16(1), H54(1), H77(2), H80(1)	0.308 ± 0.107	0.00015 ± 0.00005	C1(8), C2(13), C31(1), C66(8)	0.692 ± 0.042	0.00036 ± 0.00004
ZJTZ	H1(26), H81(3), H82(1)	0.246 ± 0.098	0.00020 ± 0.00008	C1(12), C2(12), C66(3), C71(3)	0.683 ± 0.049	0.00037 ± 0.00005
ZJWZ	H1(30)	0.000 ± 0.000	0.00000 ± 0.00000	C66(30)	0.000 ± 0.000	0.00000 ± 0.00000

Note: Asterisks indicate *D. citri* populations in the diffusion frontier areas of HLB.

A global non-stratified analysis of molecular variance (AMOVA) was conducted on all samples to reveal the genetic structure of the population. The results indicated that 20.25% of the genetic variation occurred among populations, while the remaining 79.75% originated within populations (Table 4). The fixation index (*Fst*) value of 0.20253, which falls between 0.15 and 0.25 ($p < 0.0001$), is a key measure of population differentiation.

The neutral test showed that Tajima's *D* ($D = -2.51218$, $p < 0.001$), Fu and Li's *D* ($Fs = -8.40780$, $p < 0.02$), and Fu and Li's *F* ($Fs = -6.47071$, $p < 0.02$) all reached statistically significant levels, with $p < 0.05$. Additionally, the mismatch distribution of *D. citri* populations in the three regions were found to be monotonous (Figure 4).

Mantel test results revealed a significant correlation between genetic distance and geographical distance of *D. citri* ($R^2 = 0.085$, $p < 0.01$) (Figure 5).

(**a**)   (**b**)
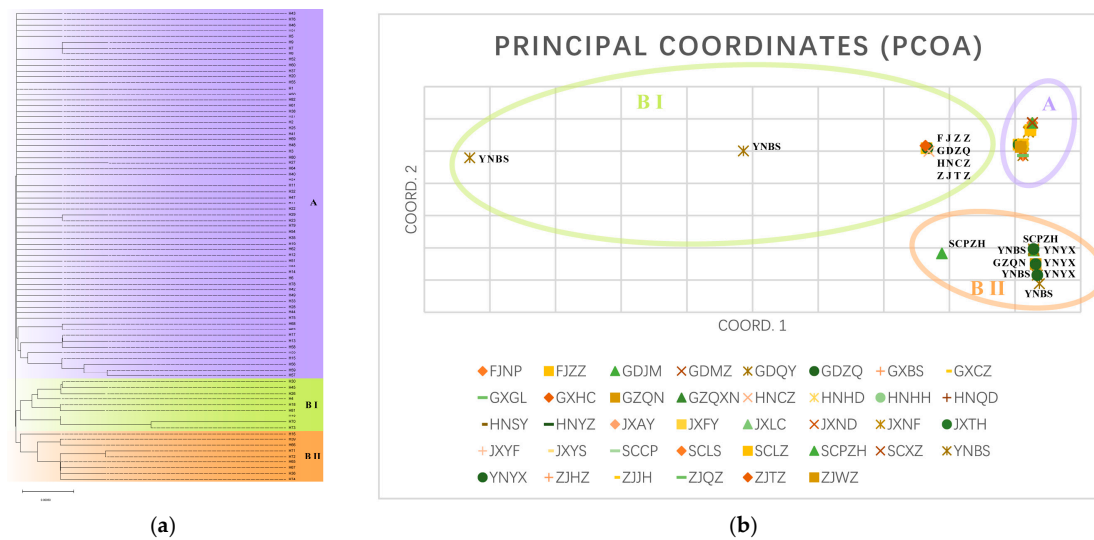
Figure 2. (**a**) Phylogenetic tree between haplotypes based on Maximum Likelihood Method of mitochondrial multi-gene concatenated sequences in *D. citri*. (**b**) PCoA based on mitochondrial multi-gene concatenated sequences of all *D. citri* populations.
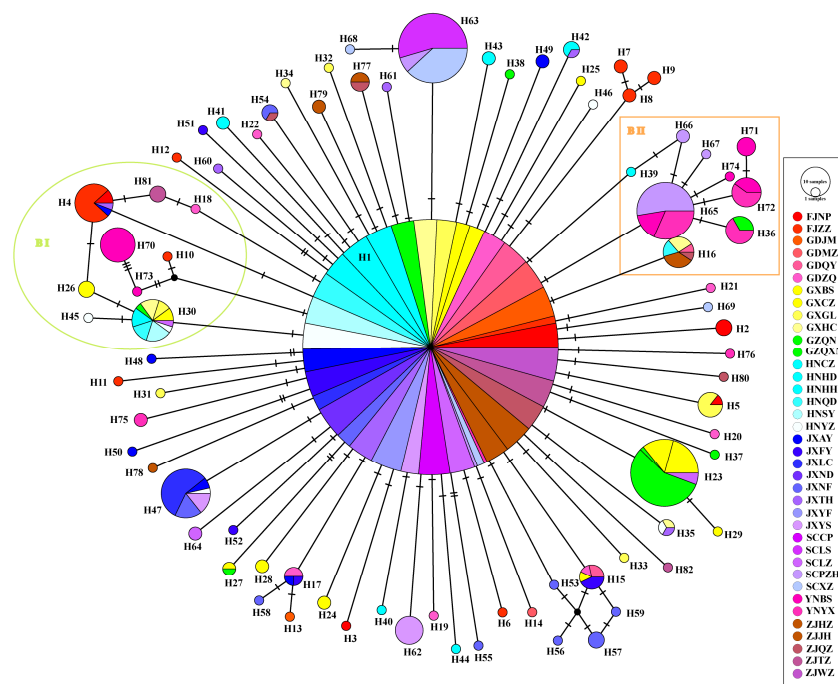

Figure 3. Haploid network of mitochondrial multi-gene concatenated sequences in *D. citri*. BI and BII rep-resent a group different from other haplotypes.

Table 4. AMOVA of mitochondrial multi-gene concatenated sequences in all populations of *D. citri*.

Source of Variation	d.f.	Sum of Squares	Variance Components	Percentage of Variation
Among populations	8	93.593	0.09191 Va	20.25%
Within populations	1131	409.302	0.36189 Vb	79.75%
Fixation Index	Fst = 0.20253		$p < 0.0001$	
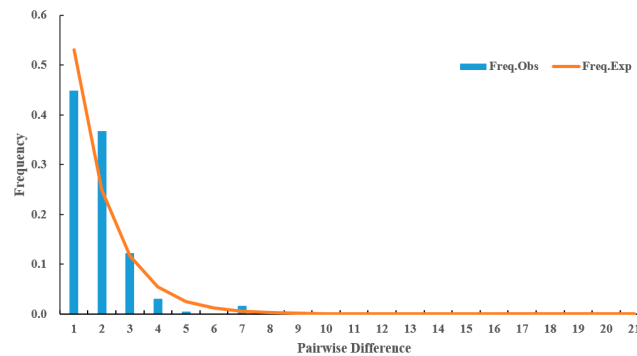
Figure 4. Mismatch distribution of mitochondria multi-gene concatenated sequences based on all *D. citri* populations.
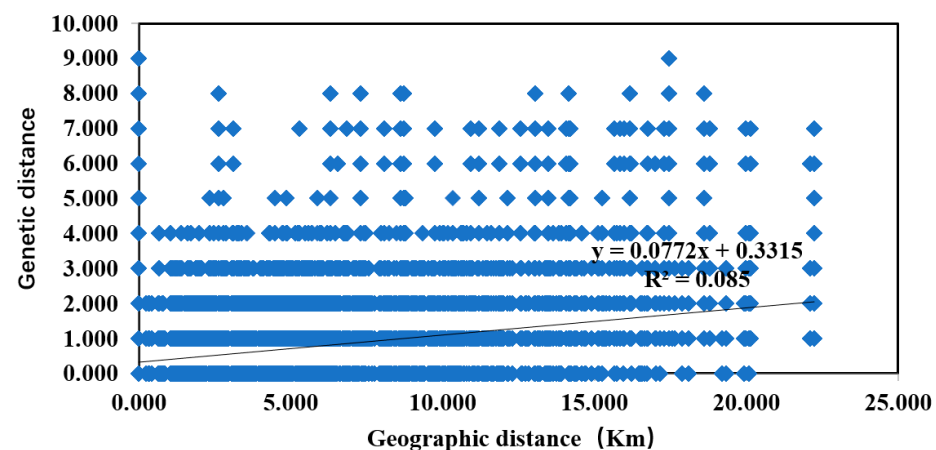
Figure 5. Relationship between genetic distance and geographic distance of *D. citri*.

3.2. Genetic Diversity and Population Structure of Two Populations of D. citri

All sampling sites were categorized into HLB diffusion frontier areas (390 individuals) and epidemic areas (750 individuals), with 28 and 70 haplotypes identified, respectively. The Hd of *D. citri* in the HLB epidemic areas was notably higher (Hd = 0.615 ± 0.021) (Table 5), likely due to the early occurrence and wide distribution of *D. citri* in this region. Ancestral haplotype H1 was the most prevalent in both regions, with frequencies of 76.67% and 61.20%, respectively. Additionally, certain regions exhibited high Hd values, such as JXLC (0.515) and JXYS (0.591) in the HLB diffusion frontier areas, and FJZZ (0.766), GXBS (0.630), GXCZ (0.745), GXGL (0.570), JXNF (0.726), SCPZH (0.540), YNBS (0.729), and YNYX (0.770) in the HLB epidemic areas. In contrast, other populations showed low Hd and π values (Table 3).

The average nucleotide difference and Ka/Ks ratio of *D. citri* in the HLB epidemic areas were higher than those in the HLB diffusion frontier areas. Similarly, genetic variation within *D. citri* populations predominated in both regions, with significantly negative results from neutral tests.

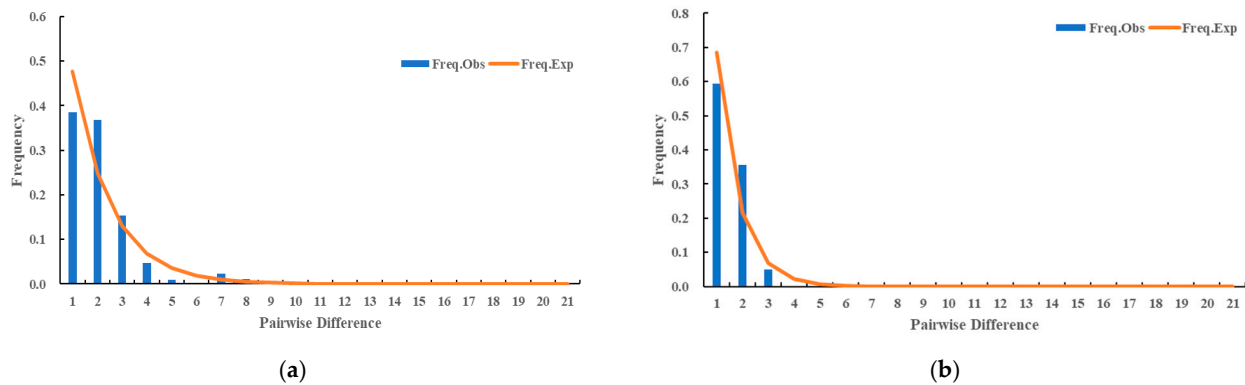Moreover, the mismatch distribution exhibited a monotonous pattern (Figure 6).

(a)

(b)

Figure 6. (**a**) Mismatch distribution of mitochondria multi-gene concatenated sequences based on *D. citri* populations in the diffusion frontier areas of HLB. (**b**) Mismatch distribution of mitochondria multi-gene concatenated sequences based on *D. citri* populations in the epidemic areas of HLB.

Table 5. Genetic diversity parameters of *D. citri* in HLB diffusion frontier and epidemic areas.

Parameters	Diffusion Frontier Area	Epidemic Area
Number of individuals	390	750
Haplotype species	28	70
Widespread haplotype	H1 (76.67%)	H1 (61.20%)
Haplotype diversity	0.406 ± 0.032	0.615 ± 0.021
Nucleotide diversity	0.00020 ± 0.00002	0.00049 ± 0.00003
Average nucleotide difference	0.458	1.092
Ka/Ks	9.29	14.00
Fst, *p*	*Fst* = 0.30930, *p* < 0.0001	*Fst* = 0.38724, *p* < 0.0001
Among populations	30.93%	38.72%
Within populations	69.07%	61.28%
Tajima's *D*, *p*	*D* = −2.17108, *p* < 0.01	*D* = −2.46049, *p* < 0.001
Fu and Li's *D*, *p*	*Fs* = −3.15833, *p* < 0.05	*Fs* = −7.36232, *p* < 0.02
Fu and Li's *F*, *p*	*Fs* = −3.33483, *p* < 0.05	*Fs* = −5.94129, *p* < 0.02

3.3. Genetic Diversity and Population Structure of Ca. C. ruddii

The *Ca.* C. ruddii multi-gene concatenated sequence alignment was 2410 bp in length (*dnaQ*: 436 bp; *rpoC*: 1189 bp; *argH*: 785 bp). The A + T content was 79.29%, indicating a notable A + T bias. A total of 64 polymorphic loci were identified, including 43 parsimony-informative loci and 21 single-variation loci. A total of 71 haplotypes (designated C1–C71) were defined (Table 3). Among these, 10 haplotypes were shared across two or more populations, while 61 were exclusive to a single population. The most widespread genotype, C1, accounted for 49.21% (561 sequences) of the total sample. Except GZQXN, SCLS, SCXZ, YNBS, YNYX, and ZJWZ, the C1 genotype was present in all other populations. Notably, unlike the *D. citri* populations, the second most abundant haplotype, C2, represented 20.79% of the *Ca.* C. ruddii samples.

Similar to *D. citri*, *Ca.* C. ruddii exhibited high Hd (0.708 ± 0.012) and low π (0.00064 ± 0.00003). The mean nucleotide difference (k) among *Ca.* C. ruddii samples was 1.531. Interestingly, more *Ca.* C. ruddii populations showed high Hd values (>0.5) compared to *D. citri* populations. Furthermore, Ka/Ks values were > 1 (2.89) for all populations.

Phylogenetic analysis revealed that the haplotypes from all populations could be grouped into two distinct groups, A and B (Figure 7a). Group A radiated outward with C1 and C2 at its core, encompassing 56 haplotypes that were widely dispersed across all sampled provinces. In contrast, group B comprised 15 haplotypes (C18, C22, C49, C50, C51, C53, C54, C55, C56, C57, C58, C59, C60, C61, C62) connected by two major haplotypes,

C18 and C22, and was predominantly found in southwest China, including the Yunnan, Guangxi, Guizhou, Sichuan, and Hunan provinces. PCoA analysis (Figure 7b) showed that while some *Ca.* C. ruddii from different populations had distinct distributions, most populations overlapped. The two groups were distinguishable in populations such as SCPZH, SCXZ, SCLS, HNSY, GXGL, YNBS, GZQN, and YNYX, which corresponded to Lineages B and A, respectively.

The haplotype network exhibited a star-shaped structure, with C1, the most frequent haplotype, at the center. C2, the second most frequent haplotype, diverged from C1 through a single mutation. It is likely that C1 and C2 represent the ancestral maternal haplotypes of the *Ca.* C. ruddii populations (Figure 8).

AMOVA analysis revealed that 56.32% of the genetic variation occurred among populations, while 43.68% occurred within populations. The primary source of genetic variation was among populations (Table 6), with the genetic variation within the *D. citri* populations being predominant. The *Fst* value: ($Fst = 0.56323 > 0.25$, $p < 0.0001$).

The neutral test results indicated that Tajima's D ($D = -2.20842$, $p < 0.01$), Fu and Li's D ($Fs = -4.21476$, $p < 0.02$), and Fu and Li's F ($Fs = -3.89280$, $p < 0.02$) were significantly negative, with $p < 0.05$. Additionally, the mismatch distribution of the total populations exhibited a monotonous pattern (Figure 9).

Moreover, the Mantel test also showed a significant correlation between the genetic and geographical distances of *Ca.* C. ruddii ($R^2 = 0.1962$, $p < 0.01$) (Figure 10).
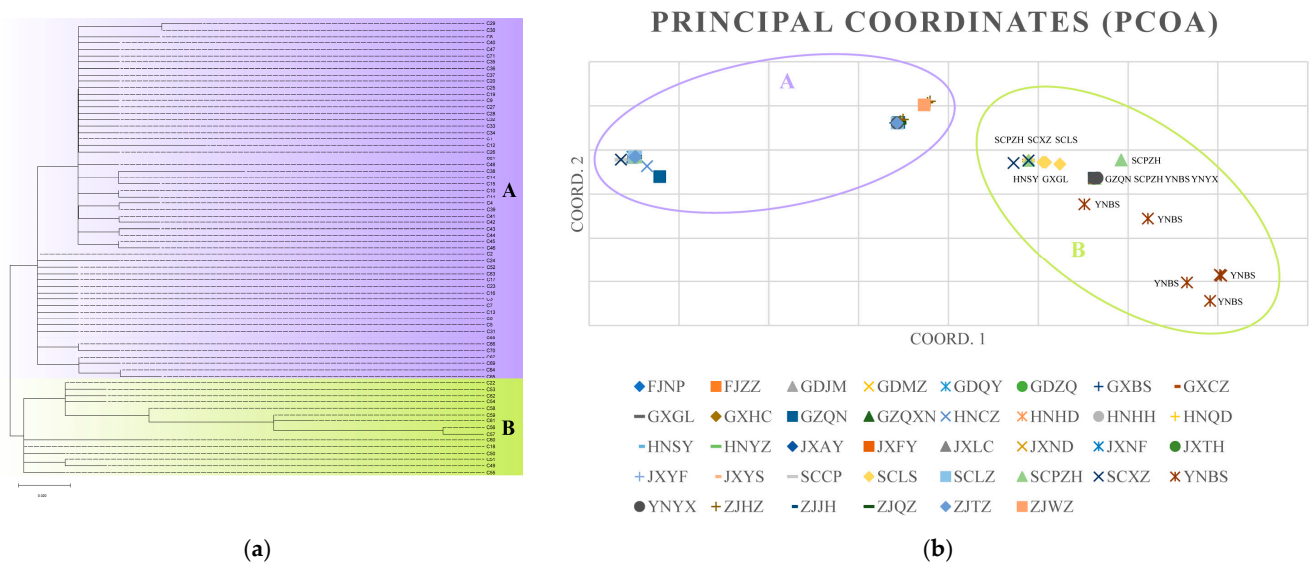

(**a**)

(**b**)

Figure 7. (**a**) Phylogenetic tree between haplotypes based on Maximum Likelihood Method of multi-gene concatenated sequences in *Ca.* C. ruddii. (**b**) PCoA based on multi-gene concatenated sequences of all *Ca.* C. ruddii populations.

Table 6. AMOVA of multi-gene concatenated sequences in all populations of *Ca.* C. ruddii.

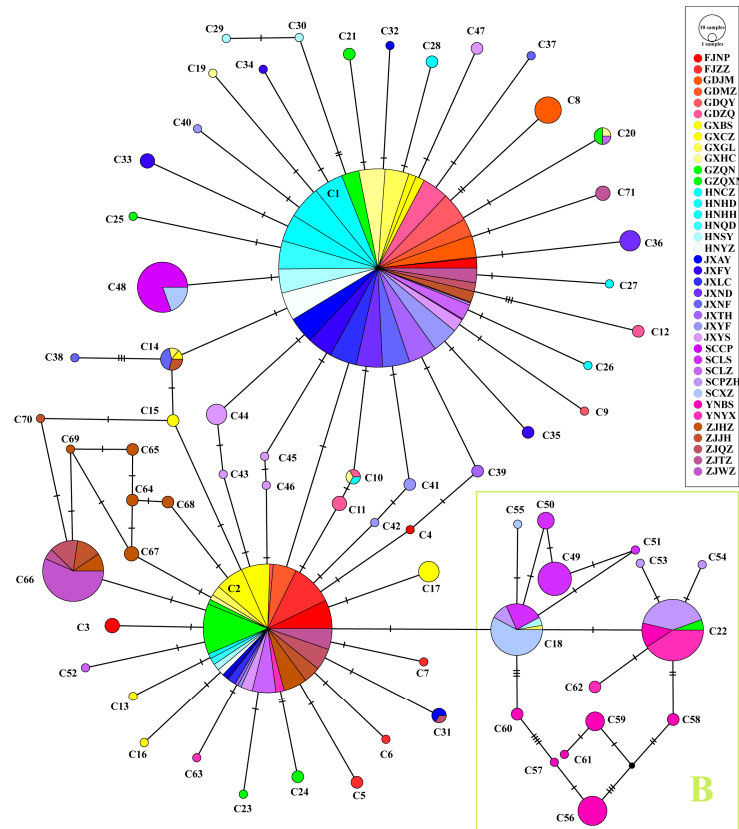| Source of Variation	d.f.	Sum of Squares	Variance Components	Percentage of Variation
Among populations	37	498.086	0.43742 Va	56.32%
Within populations	1102	373.800	0.33920 Vb	43.68%
Fixation Index	$Fst = 0.56323$		$p < 0.0001$	

Figure 8. Haploid network of multi-gene concatenated sequences in *Ca.* C. ruddii. B represents a group different from other haplotypes.
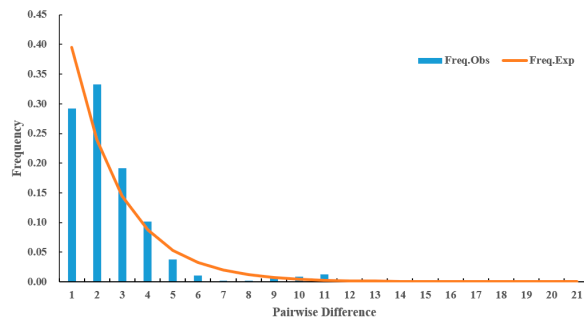

Figure 9. Mismatch distribution of multi-gene concatenated sequences based on all *Ca.* C. ruddii populations.
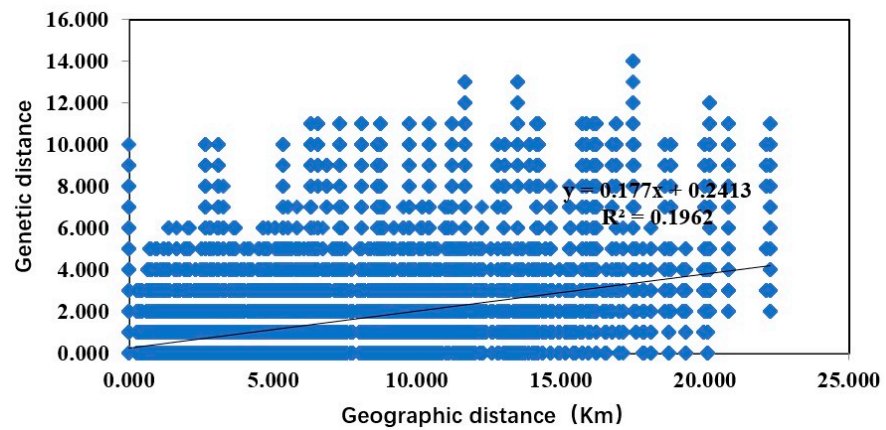

Figure 10. Relationship between genetic distance and geographic distance of *Ca.* C. ruddii.

3.4. Genetic Diversity and Population Structure of Two Populations of Ca. C. ruddii

Similar to *D. citri*, the *Ca.* C. ruddii populations can be categorized into two regions: the HLB diffusion frontier (390 individuals) and the epidemic areas (750 individuals), with 28 and 70 haplotypes identified, respectively. Both regions displayed high Hd (Hd = 0.691 ± 0.021 and 0.711 ± 0.015, respectively) (Table 7). The most prevalent haplotype in both regions was C1 (51.03% and 48.24%, respectively), likely the ancestral haplotype of the Chinese citrus woodlouse. Notably, populations in specific areas showed high Hd, such as JXYS (0.763), SCLZ (0.582), ZJHZ (0.754), ZJJH (0.743), and ZJQZ (0.692) in the HLB diffusion frontier areas, and FJNP (0.598), GDMZ (0.515), GXBS (0.621), GXCZ (0.605), GZQN (0.703), SCLS (0.628), YNBS (0.772), and ZJTZ (0.683) in the HLB epidemic areas. In contrast, populations in other areas exhibited low Hd and π values (Table 3).

The Ka/Ks ratio of the *Ca.* C. ruddii populations were higher in the HLB diffusion frontier areas, while the mean nucleotide difference was greater in the HLB epidemic areas. Variation in the HLB diffusion frontier areas primarily resulted from within populations differences, whereas variation in the epidemic areas was mainly driven by among populations dynamics. The mismatch distribution of *D. citri* populations in the two regions showed a single peak (Figure 11).
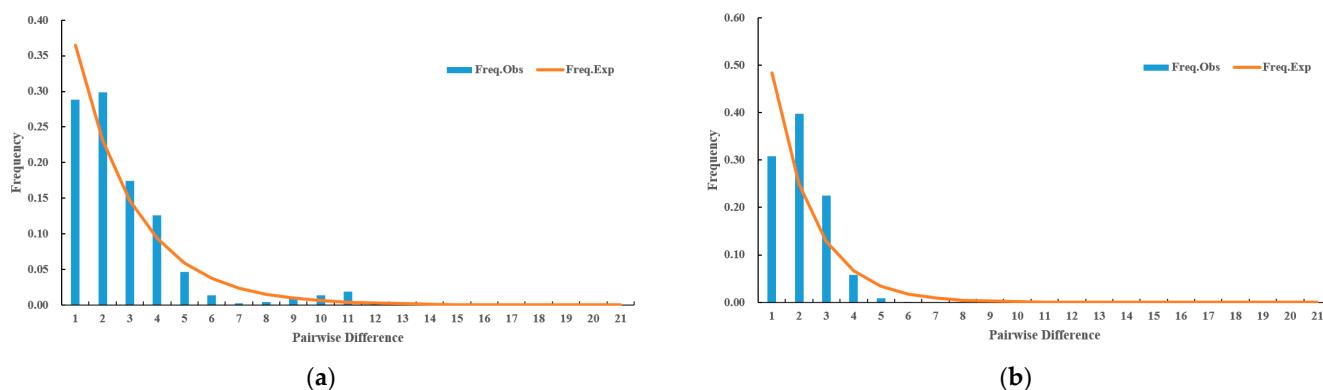

| (a) | (b) |

Figure 11. (**a**) Mismatch distribution of multi-gene concatenated sequences based on *Ca.* C. ruddii populations in the diffusion frontier areas of HLB. (**b**) Mismatch distribution of multi-gene concatenated sequences based on *Ca.* C. ruddii populations in the epidemic areas of HLB.

Table 7. Genetic diversity parameters of *Ca.* C. ruddii in HLB diffusion frontier and epidemic areas.

Parameters	Diffusion Frontier Areas	Epidemic Areas
Number of individuals	390	750
Haplotype species	28	70
Widespread haplotype	C1 (51.03%)	C1 (48.27%)
Haplotype diversity	0.691 ± 0.021	0.711 ± 0.015
Nucleotide diversity	0.00044 ± 0.00002	0.00072 ± 0.00004
Average nucleotide difference	1.067	1.741
Ka/Ks	5.76	2.44
Fst, *p*	$Fst = 0.4500$, $p < 0.0001$	$Fst = 0.59697$, $p < 0.0001$
Among populations	45.50%	59.70%
Within populations	54.50%	40.30%
Tajima's *D*, *p*	$D = -1.21063$, $p > 0.10$	$D = -2.05047$, $p < 0.05$
Fu and Li's *D*, *p*	Fs = -1.64401, $p > 0.10$	Fs = -4.00935, $p < 0.05$
Fu and Li's *F*, *p*	Fs = -1.57510, $p = 0.10 > 0.05$	Fs = -3.72869, $p < 0.02$

4. Discussion

Phylogeographic studies of *D. citri* have predominantly focused on mitochondrial genes [2,29,30], such as *COI* and *Cytb*, in order to reconstruct species invasion routes and evolutionary trends [53]. This study found low genetic diversity in *D. citri*, likely due to limited sequence variation in the mitochondrial genes *COI*, *ND5*, and *Cytb*. Specifically, despite that both *Cytb* and *ND5* are mitochondrial genes, they exhibited significantly less sequence variation than *COI*. This may be linked to small population size and/or a bottleneck effect [54]. The nuclear gene of *D. citri* is maternally inherited [55], evolving slowly. Consequently, recently separated populations often exhibit high genetic similarity [56], further supporting the idea that haplotype and genetic diversity in *D. citri* are lower in the HLB diffusion frontier areas compared to those in HLB epidemic areas. Another possibility is that Wolbachia infection may reduce mtDNA mutations [30]

Among all *D. citri* and its endosymbionts populations, we observed consistent genetic patterns. Some populations exhibited high Hd, suggesting they may have experienced population bottlenecks followed by rapid growth and mutation accumulation. Conversely, other populations showed low Hd and π, indicating potential bottleneck effects or founder events in their evolutionary history. Additionally, a KA/KS ratio > 1 was observed in two populations, thereby indicating that the *D. citri* and its endosymbionts were naturally selected. The *Fst* values for all populations exceeded 0.15, indicating a high degree of genetic differentiation within the *D. citri* and endosymbiont populations. Neutrality tests, including Tajima's *D*, Fu and Li's *D*, and Fu and Li's *F*, yielded statistically significant results ($p < 0.05$), suggesting the absence of neutral mutations and pointed towards a recent population expansion [51,52]. The monotonous distribution of the population mismatch further supports the hypothesis of a recent population expansion. Lastly, Mantel test results showed a significant correlation between genetic and geographical distances, indicating that gene flow in these populations may be influenced by geographic factors.

Parasites are valuable tools for inferring the evolutionary history of their hosts [57]. Vertically transmitted parasites are particularly informative, as they preserve the pedigree history of their hosts most effectively [58,59]. Some microorganisms, closely linked to their hosts' evolutionary history, provide insights into host origins and migrations [59]. Endosymbionts, in particular, exhibit strict vertical transmission, closely mirroring the evolutionary trajectories of their insect hosts [60]. For example, the symbiotic relationship between *Ca.* C. ruddii and *D. citri* is well-established through systematic development [61]. Analyzing the genomic characteristics of *Ca.* C. ruddii offers a useful tool for understanding the evolutionary history of its host [62], revealing a pattern of parallel evolution. Notably, haplotype network and population structure analyses show genetic distinctions between the citrus canker pathogen and its endosymbionts, *Ca.* C. ruddii, consistent with prior research [63]. This discrepancy may result from the faster evolution of endosymbionts' genes compared to their hosts, facilitating the inference of evolutionary and geographical relationships among recently differentiated host species [64]. Differences in generation time, mutation rates, or the significance of interactions may cause endosymbionts to evolve more rapidly than their hosts [65,66]. Additionally, host dispersal plays a pivotal role in determining gene flow and genetic structure among symbiotic populations [67,68].

In the haplotype network diagram of *Ca.* C. ruddii, the two predominant haplotypes were C1 and C2. These haplotypes were present in nearly all sampling sites, except for a few distributions in Sichuan and Yunnan provinces, where ZJWZ was absent. Additionally, C2 and C1 differed by only one mutation base, suggesting that they could be considered ancestral haplotypes of *Ca.* C. ruddii. The haplotype network diagram of *Ca.* C. ruddii can be categorized into two distinct groups, namely Group A and Group B. Notably, the 15 haplotypes comprising Group B are predominantly concentrated in southwestern China,

suggesting the formation of a unique subpopulation of *Ca.* C. ruddii in this region. By synthesizing insights from this study with previous research advancements, it is speculated that southwest China is one of the diffusion points of *Ca.* C. ruddii in China. The absence of common haplotypes C1 and C2 in Sichuan and Yunnan provinces suggests that the primary source of *Ca.* C. ruddii in these regions are neighboring areas, such as Guizhou and Guangxi, although artificial transmission cannot be ruled out [38]. Notably, all 30 individuals from ZJWZ belong to haplotype C66, unique to Zhejiang province, with only one base variation from C66 and C2. This indicates that the Zhejiang *Ca.* C. ruddii populations have evolved a unique haplotype adapted to the local environment [69]. In Fujian, Guangdong, Hunan, and Guangxi, the haplotypes are primarily C1 and C2, which suggests these regions are the origin of *Ca.* C. ruddii diffusion, consistent with the findings of Luo et al. [30]. Regarding the haplotype network structure of *D. citri*, H1 was the most widely distributed and the common haplotype. Except for the SCCP and SCLZ populations, the haplotype structure of the Sichuan and Yunnan provinces are similar to that of *Ca.* C. ruddii, where the number of ancestral haplotypes is small, and the dominant haplotypes are H63 and H65. These two haplotypes are found only in Sichuan and Yunnan. Geographical distribution is considered one of the most critical factors influencing the population genetics of species [70]. However, the GZQXN haplotypes are all H23, and apart from GZQXN, H23 is found only in Guangxi and SCLZ, suggesting that the *D. citri* in the GZQXN area originated from Guangxi.

Currently, HLB has been reported in 11 provinces (autonomous regions) and 365 counties (cities and districts) in China (moa.gov.cn). Notably, data from 2022 reveal that HLB had already been detected in Xinning County, Shaoyang City, Hunan Province, as early as 2021 [31]. This suggests that the distribution of *D. citri* is gradually shifting northward, leading to the northward spread of both HLB and *D. citri* [71–74]. This study identifies specific areas as HLB diffusion frontier areas, defined as the northernmost regions of provinces where HLB has been reported, according to the Ministry of Agriculture and Rural Affairs of China. Additionally, these areas also include regions where *D. citri* were detected during the study period. The primary strategy for controlling the spread of HLB is to prevent and manage *D. citri*, the transmission vector. In this study, *D. citri* samples were collected from both HLB-affected areas and diffusion frontiers. Their mitochondrial DNA and the diversity of primary endosymbionts were analyzed to provide valuable data.

The results showed that the genetic diversity of *D. citri* and *Ca.* C. ruddii in the HLB diffusion frontier areas was lower than in the HLB epidemic areas. This is attributed to the shorter colonization time and lower evolutionary degree of populations in the HLB diffusion frontier areas. The population variation of *Ca.* C. ruddii in these areas were primarily within the populations, indicating a direct correlation to its single origin. Notably, 10 common haplotypes (H1, H15, H16, H17, H23, H30, H42, H47, H54, and H63) were shared between *D. citri* in the HLB diffusion frontier and epidemic areas, providing key evidence of the genetic relationship between the two regions. Additionally, *D. citri* in the HLB diffusion frontier areas of Zhejiang Province may be transmitted by GDQY via JXNF, while *D. citri* in Hunan Province may be transmitted by Guangxi via HNYZ and HNCZ. Similarly, *D. citri* in the HLB diffusion frontier areas of Jiangxi Province may be transmitted by Guangdong via JXAY, JXND, and JXNF. Additionally, SCXZ *D. citri* may be transmitted by SCPZH via SCLS. The study also indicated that the evolution of *Ca.* C. ruddii is more conservative than that of *D. citri*. Eight common haplotypes (C1, C2, C14, C18, C20, C31, C48, and C66) were shared between *D. citri* in the HLB diffusion frontier and *Ca.* C. ruddii in the HLB epidemic areas. Based on these findings, it is speculated that *Ca.* C. ruddii in the HLB diffusion frontier areas of Zhejiang Province spread from Guangxi through Jiangxi, with some spread occurring through the ZJWZ and ZJTZ epidemic areas. Similarly, *Ca.*

C. ruddii in the HLB diffusion frontier areas of Sichuan Province may be transmitted by SCPZH and SCLS in Guangxi.

It is generally hypothesized that there are three invasion routes for *D. citri* in China. The first route involves an eastward spread from Yunnan Province to Sichuan, Guizhou, and Guangxi. The second route entails a northeastward expansion from Guangdong Province to Fujian, Jiangxi, and Zhejiang. The third route is a northwestward spread from Guangdong Province to Guangxi, Guizhou, and Hunan. This aligns with the route predicted by Luo et al. [30]. Therefore, these data suggest multiple introduction events in China [75].

The neutral test and single-peak mismatch distributions yielded significantly negative results for both *D. citri* and *Ca.* C. ruddii populations, as well as for both the HLB diffusion frontier and epidemic areas. These findings indicate historical population expansion. The two key factors that may have influenced this expansion are the growth of citrus plantation areas [69] and environmental changes [76–78].

In assessing potential suitable areas for HLB and *D. citri*, it was found that the Chongqing and Hubei provinces offer suitable habitats for *D. citri* [71–74], posing a serious threat to China's citrus industry. Effective HLB management should not only focus on prevention and control within epidemic areas but also include comprehensive surveillance of *D. citri*. This involves determining their annual distribution and eradicating *D. citri* from areas where HLB has not yet occurred, in order to prevent further northward expansion of the disease.

5. Conclusions

We investigated the genetic diversity of *D. citri* and *Ca.* C. ruddii in both the frontier and epidemic areas of HLB in China. The analysis revealed that both species exhibited high Hd, but low π in China. Interestingly, similar genetic structures were observed across diverse regions, including both the frontier and epidemic areas of HLB. Based on the haplotype distribution across regions, we propose three potential invasion routes: (1) Guangdong spreading northeast, (2) Guangdong spreading west and northwest, and (3) Yunnan spreading east. Additionally, we found that *D. citri* populations in the frontier areas of HLB primarily originate from nearby epidemic areas, although the possibility of artificial transmission cannot be ruled out. Therefore, this study aims to provide valuable insights into the potential northward expansion of *D. citri*, facilitating better understanding and management of this devastating citrus pest.

Author Contributions: Conceptualization, J.Y., A.-J.H., J.Z. and L.Y.; methodology, J.Y., A.-J.H., J.Z. and L.Y.; software, J.Y., P.Y., X.L. and H.L.; investigation, J.Y., P.Y. and X.L.; formal analysis, J.Y., A.-J.H., J.Z. and L.Y.; data curation, J.Y., A.-J.H. and J.Z.; supervision and funding acquisition, L.Y.; writing—original draft preparation, J.Y.; writing—review and editing, J.Y. and L.Y. All authors have read and agreed to the published version of the manuscript.

Institutional Review Board Statement: Not applicable.

Data Availability Statement: The data presented in this study are available in an article.

Conflicts of Interest: The authors declare no conflicts of interest.

References

1. Garnier, M.; Danel, N.; Bové, J.M. The Greening Organism is a Gram-Negative Bacterium. *Proc. Conf. Int. Organ. Citrus Virol.* **1984**, *9*, 115–124. [CrossRef]
2. Jagoueix, S.; Bové, J.M.; Garnier, M. The phloem-limited bacterium of greening disease of citrus is a member of the alpha subdivision of the Proteobacteria. *Int. J. Syst. Bacteriol.* **1994**, *44*, 79–386. [CrossRef]

3. Garnier, M.; Jagoueix-Eveillard, S.; Cronje, P.R.; Le-Roux, H.F.; Bové, J.M. Genomic characterization of a Liberibacter present in an ornamental rutaceous tree, *Calodendrum capense*, in the Western Cape Province of South Africa. Proposal of 'Candidatus Liberibacter africanus subsp. capensis'. *Int. J. Syst. Evol. Microbiol.* **2000**, *50*, 19–2125. [CrossRef]

4. Coletta-Filho, H.D.; Takita, M.A.; Targon, M.L.P.N.; Machado, M.A. Analysis of 16S rDNA Sequences from Citrus Huanglongbing Bacteria Reveal a Different "*Candidatus* Liberibacter" Strain Associated with Citrus Disease in São Paulo. *Plant Dis.* **2005**, *89*, 8–852. [CrossRef]

5. Teixeira, D.C.; Ayres, J.; Kitajima, E.W.; Danet, L.; Jagoueix-Eveillard, S.; Saillard, C.; Bové, J.M. First Report of a Huanglongbing-Like Disease of Citrus in Sao Paulo State, Brazil and Association of a New Liberibacter Species, *Candidatus* Liberibacter americanus, with the Disease. *Plant Dis.* **2005**, *89*, 107. [CrossRef] [PubMed]

6. Bové, J.M. Huanglongbing: A destructive, newly-emerging, century-old disease of citrus. *J. Plant Pathol.* **2006**, *88*, 7–37.

7. Zetian, J. Citrus wilt disease (Yu Bao). *Taiwan. Agric. News.* **1913**, *83*, 903–914.

8. Reinking, O.A. Diseases of economic plants in Southern China. *Philipp. Agric.* **1919**, *8*, 109–135.

9. Hu, B.; Rao, M.J.; Deng, X.X.; Pandey, S.S.; Hendrich, C.; Ding, F.; Wang, N.; Xu, Q. Molecular signatures between citrus and *Candidatus* Liberibacter asiaticus. *PLoS Pathog.* **2021**, *17*, e1010071. [CrossRef]

10. Zhou, C.Y. The status of citrus Huanglongbing in China. *Trop. Plant Pathol.* **2020**, *45*, 279–284. [CrossRef]

11. Hodkinson, I.D.; White, I.M. The Neotropical Psylloidea (Homoptera: Insecta): An annotated check list. *J. Nat. Hist.* **1981**, *15*, 491–523. [CrossRef]

12. Kuwayama, S. Transactions of the Sapporo Natural History Society. *Die Psylliden Japans.* **1908**, *2*, 149–189.

13. Hoffmann, W.E. *Diaphorina citri* Kuw. (Homoptera: Chermidae), a Citrus Pest in Kwangtung. *Lingnan Sci. J.* **1936**, *15*, 127–132.

14. Oxford University Press. Terceiro Catalogo Dos Insectos Que Vivem Nas Plantas Do Brasil. *Univ. Complut. Madr. Serv. Publ.* **1936**, *37*, 469–475.

15. Yao, T.S.; Zhou, Y.; Zhou, C.Y. Research progress on occurrence and control of Asian citrus psyllid. *J. Fruit Trees.* **2018**, *35*, 1413–1421.

16. Halbert, S.E.; Manjunath, K.L. Asian citrus psyllids (Sternorrhyncha: Psyllidae) and greening disease in citrus: A literature review and assessment of risk in Florida. *Fla. Entomol.* **2004**, *87*, 330–353. [CrossRef]

17. Hall, G.D.; Richardson, L.M.; Ammar, E.; Halbert, S.E. Asian citrus psyllid, *Diaphorina citri*, vector of citrus huanglongbing disease. *Entomol. Exp. Appl.* **2013**, *146*, 207–223. [CrossRef]

18. Halbert, S.E.; Nu-Nez, C.A. Distribution of the Asian citrus psyllid, *Diaphorina citri* kuwayama (Rhynchota: Psyllidae) in the Caribbean basin. *Fla. Entomol.* **2004**, *87*, 401–402. [CrossRef]

19. Boykin, L.M.; Barro, P.D.; Hall, D.G.; Hunter, W.B.; Mckenzie, C.L.; Powell, C.A.; Shatters, R.G. Overview of worldwide diversity of *Diaphorina citri* Kuwayama mitochondrial cytochrome oxidase 1 haplotypes: Two Old World lineages and a New World invasion. *Bull. Entomol. Res.* **2012**, *102*, 573–582. [CrossRef]

20. Richard, W.H.P.; Jawwad, A.Q.I.; Philip, A.S. Citrus flushing patterns, *Diaphorina citri* (Hemiptera: Psyllidae) populations and parasitism by *Tamarixia* Radiata (Hymenoptera: Eulophidae) in Puerto Rico. *Fla. Entomol.* **2008**, *91*, 36–42.

21. Halbert, S.E.; Manjunath, K.L.; Ramadugu, C.; Brodie, M.W.; Webb, S.E.; Lee, R.F. Trailers Transporting Oranges to Processing Plants Move Asian Citrus Psyllids. *Fla. Entomol.* **2010**, *93*, 33–38. [CrossRef]

22. Garnier, M.; Jagoueix, S.; Toorawa, P.; Grisoni, M.; Mallessard, R.; Dookun, A.; Saumtally, S.; Autrey, J.C.; Bobe, J.J. Both Huanglongbing (Greening) Liberobacter Species Are Present in Mauritius and Reunion. *Proc. Conf. Int. Organ. Citrus Virol.* **1996**, *13*, 392–394. [CrossRef]

23. Guillemaud, T.; Ciosi, M.; Lombaert, E.; Estoup, A. Biological invasions in agricultural settings: Insights from evolutionary biology and population genetics. *C. R. Biol.* **2010**, *334*, 237–246. [CrossRef]

24. De-León, J.S.; Setamou, M.; Gastaminza, G.A.; Buenahora, J.; Cáceres, S.; Yamamoto, P.T.; Bouvet, J.P.; Logarzo, G.A. Two separate introductions of Asian citrus psyllid populations found in the American continents. *Ann. Entomol. Soc. Am.* **2011**, *104*, 1392–1398. [CrossRef]

25. Fuentes, A.; Braswell, W.E.; Ruiz-Arce, R.; Racelis, A. Genetic variation and population structure of *Diaphorina citri* using cytochrome oxidase I sequencing. *PLoS ONE* **2018**, *13*, e0198399. [CrossRef]

26. Lashkari, M.; Manzari, S.; Sahragard, A.; Malagnini, V.; Boykin, L.M.; Hosseini, R. Global genetic variation in the Asian citrus psyllid, *Diaphorina citri* (Hemiptera: Liviidae) and the endosymbiont Wolbachia: Links between Iran and the USA detected. *Pest Manage. Sci.* **2014**, *70*, 1033–1040. [CrossRef] [PubMed]

27. Guidolin, A.S.; Fresia, P.; Cônsoli, F.L. The genetic structure of an invasive pest, the Asian citrus psyllid *Diaphorina citri* (Hemiptera: Liviidae). *PLoS ONE* **2014**, *9*, e115749. [CrossRef]

28. Simon, C.; Frati, F.; Beckenbach, A.; Crespi, B.; Liu, H.; Flook, P. Evolution, weighting, and phylogenetic utility of mitochondrial gene sequences and a compilation of conserved polymerase chain reaction primers. *Ann. Entomol. Soc. Am.* **1994**, *87*, 651–701. [CrossRef]

29. Zhang, C.; Xiong, X.; Liu, X.; Zou, Z.; Xin, T.; Wang, J.; Xia, B. *Diaphorina citri* (Hemiptera: Psylloidea) in China: Two invasion routes and three transmission paths. *J. Econ. Entomol.* **2019**, *112*, 1418–1427. [CrossRef]

30. Luo, Y.; Agnarsson, I. Global mtDNA genetic structure and hypothesized invasion history of a major pest of citrus, *Diaphorina citri* (Hemiptera: Liviidae). *Ecol. Evol.* **2018**, *8*, 257–265. [CrossRef]

31. Huang, A.J.; Ma, J.Y.; Yang, J.; Chen, B.; Zhou, J.; Yi, L. Genetic diversity and population structure of the Asian citrus psyllid in China. *J. Insect Sci.* **2024**, *24*, 2. [CrossRef]

32. Cui, X.J.; Liu, K.H.; Huang, J.; Fu, S.M.; Chen, Q.D.; Liu, X.; Zhou, C.Y.; Wang, X.F. Population diversity of "*Candidatus* Liberibacter asiaticus" and *Diaphorina citri* in Sichuan: A case study for Huanglongbing monitoring and interception. *Plant Dis.* **2021**, *106*, 1632–1638. [CrossRef] [PubMed]

33. Santiago-Rosario, L.Y.; Faldyn, M.J.; Martínez-Cález, E.L.; Rivera-Marchand, B. The Invasion History of *Diaphorina citri* (Hemiptera: Liviidae) in Puerto Rico: Past, Present, and Future Perspectives. *Environ. Entomol.* **2023**, *52*, 259–269. [CrossRef] [PubMed]

34. Zhang, N.; Zhao, M.; Wang, G.H. Research progress on insect symbiotic microorganisms in disease and pest control. *J. Plant Prot.* **2022**, *49*, 220–230.

35. Baumann, P. Biology of bacteriocyte-associated endosymbionts of plant sapsucking insects. *Annu. Rev. Microbiol.* **2005**, *59*, 155–189. [CrossRef]

36. Nachappa, P.; Levy, J.; Pierson, E.; Tamborindeguy, C. Diversity of endosymbionts in the potato psyllid, *Bactericera cockerelli* (Triozidae), vector of zebra chip disease of potato. *Curr. Microbiol.* **2011**, *62*, 1510–1520. [CrossRef] [PubMed]

37. Nakabachi, A.; Yamashita, A.; Toh, H.; Ishikawa, H.; Dunbar, H.E.; Moran, N.A.; Hattori, M. The 160-Kilobase Genome of the Bacterial Endosymbiont Carsonella. *Science* **2006**, *314*, 267. [CrossRef]

38. Wang, Y.; Xu, C.; Tian, M.; Deng, X.; Cen, Y.; He, Y. Genetic diversity of *Diaphorina citri* and its endosymbionts across east and southeast Asia. *Pest Manage. Sci.* **2017**, *73*, 2090–2099. [CrossRef] [PubMed]

39. Wu, F.N.; Dai, Z.H.; Shi, M.; Huang, J.J.; Zhu, H.; Zheng, Y.Z.; Chen, Z.K.; Li, X.H.; Deng, X.L.; Fox, E.G.P. Tracking the geographical distribution of the Asian citrus psyllid *Diaphorina citri* throughout China using mitogenomes and endosymbionts. *J. Pest Sci.* **2024**, 1–13. [CrossRef]

40. Zhang, J.H.; Liu, Q.; Dai, L.Y.; Zhang, Z.J.; Wang, Y.S. Pan-Genome Analysis of Wolbachia, Endosymbiont of *Diaphorina citri*, Reveals Independent Origin in Asia and North America. *Int. J. Mol. Sci.* **2024**, *25*, 4851. [CrossRef] [PubMed]

41. Ajene, I.J.; Khamis, F.; Ballo, S.; Pietersen, G.; Asch, B.V.; Seid, N.; Azerefegne, F.; Ekesi, S.; Mohamed, S. Detection of Asian Citrus Psyllid (Hemiptera: Psyllidae) in Ethiopia: A New Haplotype and its Implication to the Proliferation of Huanglongbing. *J. Econ. Entomol.* **2020**, *113*, 1640–1647. [CrossRef] [PubMed]

42. Oke, A.O.; Oladigbolu, A.A.; Kunta, M.; Alabi, O.J.; Sétamou, M. First report of the occurrence of Asian citrus psyllid *Diaphorina citri* (Hemiptera: Liviidae), an invasive species in Nigeria, West Africa. *Sci. Rep.* **2020**, *10*, 9418. [CrossRef]

43. Swindell, S.R.; Plasterer, T.N. Seqman. Contig assembly. *Methods Mol. Biol.* **1997**, *70*, 75–89. [PubMed]

44. Kumar, S.; Stecher, G.; Li, M.; Knyaz, C.; Tamura, K. MEGA X: Molecular Evolutionary Genetics Analysis across Computing Platforms. *Mol. Biol. Evol.* **2018**, *35*, 1547–1549. [CrossRef]

45. Librado, P.; Rozas, J. DnaSP v5: A software for comprehensive analysis of DNA polymorphism data. *Bioinformatics* **2009**, *25*, 1451–1452. [CrossRef] [PubMed]

46. Excoffier, L.; Lischer, H.E. Arlequin suite ver 3.5: A new series of programs to perform population genetics analyses under Linux and Windows. *Mol. Ecol. Resour.* **2010**, *10*, 564–567. [CrossRef] [PubMed]

47. Leigh, J.W.; Bryant, D. PopART: Full-Feature Software for Haplotype Network Construction. *Methods Ecol. Evol.* **2015**, *6*, 1110–1116. [CrossRef]

48. Clement, M.; Posada, D.; Crandall, K.A. TCS: A computer program to estimate gene genealogies. *Mol. Ecol.* **2000**, *9*, 1657–1659. [CrossRef] [PubMed]

49. Mantel, N. The detection of disease clustering and a generalized regression approach. *Cancer Res.* **1967**, *27*, 209–220.

50. Peakall, R.; Smouse, P.E. GenAIEx 6.5: Genetic analysis in Excel. Population genetic software for teaching and research--an update. *Bioinformatics* **2012**, *28*, 2537–2539. [CrossRef] [PubMed]

51. Dalmon, A.; Halkett, F.; Granier, M.; Delatte, H.; Peterschmitt, M. Genetic structure of the invasive pest *Bemisia tabaci*: Evidence of limited but persistent genetic differentiation in glasshouse populations. *Heredity* **2008**, *100*, 316–325. [CrossRef]

52. Nei, M.; Maruyama, T.; Chakraborty, R. The Bottleneck effect and genetic variability in populations. *Evolution* **1975**, *29*, 1–10. [CrossRef] [PubMed]

53. Searle, J.B. Phylogeography—The History and Formation of Species. *Heredity* **2000**, *85*, 201–202. [CrossRef]

54. Barbosa, N.C.C.P.; De, F.S.; Morales, A.C. Distinct genetic structure in populations of *Chrysoperla externa* (Hagen) (Neuroptera, Chrysopidae) shown by genetic markers ISSR and *COI* gene. *Rev. Bras. Entomol.* **2014**, *58*, 203–211. [CrossRef]

55. Tajima, F. Statistical method for testing the neutral mutation hypothesis by DNA polymorphism. *Genetics* **1989**, *123*, 585–595. [CrossRef]

56. Fu, Y.X. Statistical tests of neutrality of mutations against population growth, hitchhiking and background selection. *Genetics* **1997**, *147*, 915–925. [CrossRef]

57. Whiteman, N.K.; Parker, P.G. Using parasites to infer host population history: A new rationale for parasite conservation. *Anim. Conserv.* **2005**, *8*, 175–181. [CrossRef]

58. Clay, T. Some problems in the evolution of a group of ectoparasites. *Evolution* **1949**, *3*, 279–299. [CrossRef] [PubMed]

59. Thierry, W.; Axel, M.; Mark, A. Deciphering host migrations and origins by means of their microbes. *Mol. Ecol.* **2005**, *14*, 3289–3306.

60. Bennett, G.M.; Moran, N.A. The advantages and perils of an evolutionary rabbit hole. *Proc. Natl. Acad. Sci. USA* **2015**, *112*, 10169–10176. [CrossRef]

61. Thao, M.L.; Moran, N.A.; Abbot, P.; Brennan, E.B.; Burckhardt, D.H.; Baumann, P. Cospeciation of psyllids and their primary prokaryotic endosymbionts. *Appl. Environ. Microbiol.* **2000**, *66*, 2898–2905. [CrossRef]

62. Hall, A.A.G.; Morrow, J.L.; Fromont, C.; Steinbauer, M.J.; Taylor, G.S.; Johnson, S.N.; Cook, J.M.; Riegler, M. Codivergence of the primary bacterial endosymbiont of psyllids versus host switches and replacement of their secondary bacterial endosymbionts. *Environ. Microbiol.* **2016**, *18*, 2591–2603. [CrossRef] [PubMed]

63. Spaulding, A.W.; Von-Dohlen, C.D. Psyllid endosymbionts exhibit patterns of co-speciation with hosts and destabilizing substitutions in ribosomal RNA. *Insect Mol. Biol.* **2001**, *10*, 57–67. [CrossRef] [PubMed]

64. Moeller, A.H.; Caro–Quintero, A.; Mjungu, D.; Georgiev, A.V.; Lonsdorf, E.V.; Muller, M.N.; Pusey, A.E.; Peeters, M.; Hahn, B.H.; Ochman, H. Cospeciation of gut microbiota with hominids. *Science* **2016**, *353*, 380–382. [CrossRef] [PubMed]

65. Moran, N.A.; Dohlen, C.D.; Baumann, P. Faster evolutionary rates in endosymbiotic bacteria than in cospeciating insect hosts. *J. Mol. Evol.* **1995**, *41*, 727–731. [CrossRef]

66. Bergstrom, C.T.; Lachmann, M. The Red King effect: When the slowest runner wins the coevolutionary race. *Proc. Natl. Acad. Sci. USA* **2003**, *100*, 593–598. [CrossRef]

67. Blouin, M.S.; Yowell, C.A.; Courtney, C.H.; Dame, J.B. Host movement and the genetic structure of populations of parasitic nematodes. *Genetics* **1995**, *141*, 1007–1014. [CrossRef]

68. Criscione, C.D.; Poulin, R.; Blouin, M.S. Molecular ecology of parasites: Elucidating ecological and microevolutionary processes. *Mol. Ecol.* **2005**, *14*, 2247–2257. [CrossRef]

69. Meng, L.X.; Wang, Y.M.; Wei, W.H.; Zhang, H.Y. Population genetic structure of *Diaphorina citri* Kuwayama (Hemiptera: Liviidae): Host-driven genetic differentiation in China. *Sci. Rep.* **2018**, *8*, 1473. [CrossRef]

70. Yang, X.Q.; Ye, Q.T.; Xin, T.R.; Zou, Z.W.; Xia, B. Population genetic structure of *Cheyletus malaccensis* (Acari: Cheyletidae) in China based on mitochondrial *COI* and 12S rRNA genes. *Exp. Appl. Acarol.* **2016**, *69*, 117–128. [CrossRef] [PubMed]

71. Wang, R.L.; Yang, H.; Luo, W.; Wang, M.T.; Lu, X.L.; Huang, T.T.; Zhao, J.P.; Li, Q. Predicting the potential distribution of the Asian citrus psyllid, *Diaphorina citri* (Kuwayama), in China using the MaxEnt model. *PeerJ* **2019**, *7*, e7323. [CrossRef] [PubMed]

72. Yao, J.M.; Liu, D.; Duan, L.C.; Cai, Z. Estimation of the potential impact range of citrus psylla in China under the CMIP6 climate change scenario. *Chin. J. Agrometeorol.* **2021**, *42*, 1031–1041.

73. Zhao, Y.; Wang, J.G.; Chen, C.; Mao, Q.Y.; Huang, H.C.; Cai, H.; He, X.H. Study on the Potential Suitable Area of Citrus psyllid in Yunnan Based on MaxEnt Niche Model. *Yunnan Nongye Daxue Xuebao Ziran Kexue* **2022**, *37*, 61–68.

74. Liu, D.; Yao, J.M.; Yu, Y.W.; Duan, L.C.; Cai, Z. Changes of suitable areas of citrus psyllid in China under the background of climate warming. *J. Plant Prot.* **2021**, *48*, 872–881.

75. Chen, S.Y.; Su, Y.H.; Wu, S.F.; Sha, T.; Zhang, Y.P. Mitochondrial diversity and phylogeographic structure of Chinese domestic goats. *Mol. Phylogenet. Evol.* **2005**, *37*, 804–814. [CrossRef] [PubMed]

76. Yang, Y.P.; Huang, M.D.; Beattie, G.A.C.; Xia, Y.L.; Ouyang, G.C.; Xiong, J.J. Distribution, biology, ecology and control of the psyllid *Diaphorina citri* Kuwayama, a major pest of citrus: A status report for China. *Int. J. Pest Manag.* **2006**, *52*, 343–352. [CrossRef]

77. Russell, D.N.; Qureshi, J.A.; Halbert, S.E.; Stansly, P.A. Host Suitability of Citrus and Zanthoxylum Spp. for *Leuronota fagarae* Burckhardt and *Diaphorina citri* Kuwayama (Hemiptera: Psylloidea). *Fla. Entomol.* **2014**, *97*, 1481–1492. [CrossRef]

78. Boina, D.R.; Bloomquist, J.R. Chemical control of the Asian citrus psyllid and of huanglongbing disease in citrus. *Pest Manag. Sci.* **2015**, *71*, 808–823. [CrossRef] [PubMed]